

Research article

Detection of Lung Infection on CT Scan for Covid-19 Disease Using Sparrow Search Based Deep Learning Model

Brindha Samarasam¹, Kannadhasan Suriyan^{2*}, Sowparnika Balashanmugam³, Gayathri Devi Kulandasamy⁴ and Amsaveni Subramani⁴

¹*Department of Electronics and Communication Engineering, Nandha Engineering College, Erode, India*

²*Department of Electronics and Communication Engineering, Study World College of Engineering, Coimbatore, Tamilnadu, India*

³*Department of Biomedical Engineering, Nandha Engineering College, Erode, India*

⁴*Department of Electronics and Communication Engineering, Nandha College of Technology, Erode, India*

Received: 11 January 2024, Revised: 8 July 2024, Accepted: 1 November 2024, Published: 28 March 2025

Abstract

Rapid globalization of the COVID-19 virus was observed at the start of 2018. The prevention and treatment of this illness are crucial. Imaging techniques such as chest computed tomography (CT) scans and RT-PCR can be used to categorize COVID-19 more accurately in the epicenter of the outbreak. Hospital reports have indicated that RT-PCR assays are not very sensitive when used to diagnose an infection in its early stages. This has led to calls for a diagnostic method that can quickly and accurately spot the Covid-19. CT has been proven to be an effective diagnostic tool. This study investigates the application of convolutional neural networks (CNNs) for the detection of COVID-19 in lung images. We propose a bi-channel CNN that combines gray-level entropy and pre-processed images using unsharp masking. The model was trained on a dataset of lung CT scans and evaluated for its accuracy in detecting COVID-19. The outcomes demonstrated that the suggested approach aided radiotherapists in making a speedy and exact analysis of COVID-19, achieving a prediction accuracy of 93.78%, and a false-negative rate of only 6.5%. These results indicate the potential of the bi-channel CNN to enhance diagnostic accuracy and efficiency in clinical settings. This novel approach addresses the limitations of traditional RT-PCR tests and manual CT scan analysis, offering a robust tool for early and accurate COVID-19 detection. For additional verification of the quality of the projected model, we used the SARS-COV-2-CT-Scan benchmark dataset. The outcomes demonstrated that the suggested approach can aid radiotherapists in making a speedy and accurate analysis of COVID-19.

Keywords: computerized tomography; convolutional neural network; sparrow search algorithm; COVID-19 disease; CT-scan

*Corresponding author: E-mail: kannadhasan.ece@gmail.com

<https://doi.org/10.55003/cast.2025.261808>

Copyright © 2024 by King Mongkut's Institute of Technology Ladkrabang, Thailand. This is an open access article under the CC BY-NC-ND license (<http://creativecommons.org/licenses/by-nd/4.0/>).

1. Introduction

The COVID-19 pandemic has had a profound global impact, necessitating the development of reliable and efficient diagnostic methods. Traditional RT-PCR tests, although widely used, suffer from significant limitations including high false-negative rates and dependency on sample quality and testing conditions. These limitations highlight the need for alternative diagnostic approaches that can provide rapid and accurate results. CT imaging has emerged as a valuable tool for detecting COVID-19-related abnormalities in the lungs. However, manual analysis of CT scans is time-consuming, subject to inter-observer variability, and requires significant expertise. These challenges underscore the importance of automated diagnostic systems. This research proposes a bi-channel convolutional neural network (CNN) to enhance the detection of COVID-19 in lung images. By leveraging gray-level entropy images and pre-processed images using unsharp masking (UM), the bi-channel CNN aims to capture complementary features, thereby improving diagnostic accuracy. The primary aim of this study was to develop a robust and efficient diagnostic tool that could assist radiologists and healthcare professionals in making timely and accurate diagnoses, ultimately contributing to better patient outcomes and more effective management of the pandemic. The corona virus is a member of a family of RNA virus, that are found in both mammals and birds and is responsible for a variety of disorders, most commonly respiratory or enteric, and in rare cases, neural or hepatic (Rehman et al., 2021; Subramanian et al., 2022). The World Health Organization (WHO) proclaimed a global pandemic due to the alarming spread of the corona virus (COVID-19), which was believed to have originated in the Wuhan district of China (Jain et al., 2021; Swapna et al., 2022). Almost 7,961,307 people were infected as of 1st June 2020, and it was directly responsible for the deaths of 434,471 people. COVID-19 has spread to 213 different nations and territories so far. Only a few nations surpassed one million cases (Hussain et al., 2021). Droplets from a person's coughing or sneezing can easily infect others (Sadhana et al., 2021). Without a vaccine or treatment, it is crucial that infected people isolate themselves and are identified quickly to prevent the disease from spreading. RT-PCR tests can be used to diagnose the infection (Kasthuri et al., 2018). Due to a worldwide shortage of testing kits, there was only so much testing that could be done at the time. Additionally, RT-PCR is sensitive to the quality of the samples collected, and it has a high false-negative rate (Nayak et. al, 2021). Besides being a lengthy and laborious operation, sample collection suffers from a lack of resources and workers. If new cases are not reliably detected, not only will the sufferer not get the care they need, but the disease can spread to healthy people as well. Nonetheless, patients with COVID-19 can have characteristic radiographic features accurately detected using computed tomography (CT) imaging (Asnaoui et al., 2021). Hence, patients with symptoms like breathing trouble or shortness of breath can soon develop more serious problems (Yang et al., 2021; Venaktesh et al., 2022). Patients with severe illness often require ventilator assistance due to respiratory failure. Hence, even in the initial RT-PCR negative individual, a diagnosis can be obtained consistently and swiftly based on radiographic alterations (Kailasam et al., 2022).

Unfortunately, the number of patients who can benefit from CT imaging is constrained by the dearth of board-certified radiologists who can study and report on such pictures. Using the proposed automated analysis of CT imaging method, COVID-19 can be detected quickly and easily, relieving doctors of some of their duty. Although it was noted by Bhattacharyya et al. (2022) that chest X-rays also show promising results in COVID-19 detection, and it has been found that CT imaging is the better option. This is because CT imaging allows for the simultaneous capture of small bones and soft vessels.

Using CT scans as an example, artificial intelligence has the ability to greatly improve health care delivery by reshaping the standard technique of diagnosis (Diaz-Escobar et al., 2021; Biradar et al., 2022). Recently, deep learning has proven to be a useful tool for automating COVID screening and diagnosis. An efficient deep learning system can automatically and accurately diagnose an illness with the same or higher precision than human experts. When it comes to medical picture categorization, the CNN (a central paradigm of deep learning in computer vision) has shown remarkable predictive and diagnostic accuracy. In this work, we employ unsharp masking (UM), a traditional method for improving image sharpness, to extract images and boost the finer details. To improve the detection of detectable COVID-19, the proposed bi-channel CNN was trained using features extracted from gray-level entropy photos as well as those pre-processed by UM. COVID-19, caused by the SARS-CoV-2 virus, has resulted in a global pandemic, leading to significant challenges in healthcare. While RT-PCR tests are the standard diagnostic tool, they have limitations such as high false-negative rates and dependency on sample quality. CT imaging has proven to be a reliable alternative for detecting COVID-19, as it can identify characteristic features even in early stages. However, the manual analysis of CT scans is time-consuming and subject to human error, underscoring the need for automated solutions.

When it comes to patient classification, Motwani et al. (2023) showed that Dense-CNN worked well. The convergence of the CNN algorithm was also enhanced through the implementation of novel entropy. A freshly released massive dataset was used to construct and evaluate the projected model. Comparisons to established models showed that the projected approach was an improvement above the state of the art. The proposed model had a false-negative rate of only 6.5% and a prediction accuracy of 93.78%. The primary benefit of this method is the shortened time required for identifying and treating COVID-19.

For the purpose of detecting COVID-19 using CT scan pictures, Kathamuthu et al. (2023) set out to create conceptual transfer learning augmented CNN framework models. These methods were shown to be effective despite only being tested on small datasets. For the purpose of identifying instances of COVID-19 in chest CT scans, this study was proposed to investigate multiple deep transfer learning-based CNN methods. For models utilized as a starting point for this project, several performance metrics were used to compare and contrast the effectiveness of each model. For this research, the VGG16 model had the highest accuracy of any of the others tested (98.00%). Experiments that validated the suggested methodology for recognizing and monitoring COVID-19 patients yielded encouraging results. Thus, a tool can further be developed to assist primary care physicians in selecting the most effective treatment options for their patients.

In order to screen for Covid-19 pneumonia using chest CT images, Kordnoori et al. (2023) suggest a multi-task model capable of automatic classification-segmentation. Included in this model were a multi-layer perceptron for cataloguing, a single decoder for feature segmentation, and a common encoder for feature illustration. In addition to assessing the impact of image size on the model's output, the suggested model was also used to compare results from three different datasets. Both single-task and multi-task learning outcomes were analyzed. The results showed that multitasking had a noticeable impact on the enhancement of outcomes, with classification and segmentation outputs both improving to 95.40% accuracy as a result of using the technique. In addition, when compared to other methodologies, the model produced the best results. As such, the projected model was able to be used as a chief screening tool to aid primary service professionals to more effectively refer patients to specialists for further evaluation.

When it comes to automating the findings of COVID-19 in chest CT-scan pictures, Gupta & Bajaj (2023) proposed a solid framework based on deep learning-based methods.

A ten-fold holdout validation procedure was used to train, validate, and test the deep learning methods. The maximum classification accuracy of 98.91% was attained by DarkNet19. New CT images can be used to test the suggested framework and the validity of the research with simulation results using the publicly available COVID-19 CT can be demonstrated.

In light of the advancements made in transfer learning by Alhares et al. (2023), there is the need for higher generalizability across different data sets that are consistent across multiple sources. In other words, the domain of a dataset is irrelevant to the generality of the extracted representations. We used a convolutional neural network trained using the AMTLDC to forecast Covid-19 from medical pictures. We demonstrated that the AMTLDC framework was able to achieve higher accuracy than state-of-the-art transfer learning methods. In particular, we demonstrated the AMTLDC's efficacy while dealing with sparse or varying datasets. The proposed network achieved an improvement in COVID-19/SARS-CoV-2 classification accuracy of between 4-10% compared to both state-of-the-art deep learning models and traditional feature extraction methods. The model achieved competitive performance on the COVID-19 crowdsourced benchmark dataset. In the suggested model, we used a variety of receptive fields and depths to collect contextual data that might prove useful throughout the categorization process. Additionally, the model demonstrated its categorization prowess when trained and tested on a variety of data types. The choice of a bi-channel convolutional neural network (CNN) was based on the premise that combining features from different image processing techniques could enhance the model's ability to detect subtle patterns associated with COVID-19. Gray-level entropy images capture the texture and structural information of lung tissues, which are crucial for identifying abnormalities caused by COVID-19. The green component, pre-processed by unsharp masking, enhances the edges and fine details, aiding in the detection of subtle differences in lung images. By integrating these complementary features, the bi-channel CNN can more effectively distinguish between healthy and infected tissues. In our experiments, the bi-channel CNN demonstrated superior performance compared to single-channel networks. The model achieved a prediction accuracy of 93.78% and a false-negative rate of only 6.5%, outperforming traditional methods and single-channel CNNs in the detection of COVID-19 from lung CT scans. Recent studies have shown that multi-channel approaches can significantly enhance diagnostic performance (Attallah & Samir, 2022). For instance, a multi-channel model by Kathamuthu et al. (2023) achieved an accuracy of 98.00%, while our bi-channel CNN also showed competitive results, highlighting the effectiveness of combining different image processing techniques. This bi-channel approach not only provides a robust tool for current diagnostic needs but also opens avenues for further research. Future work can explore the integration of additional channels, such as spectral components or other pre-processing techniques, to further enhance diagnostic accuracy and robustness.

2. Materials and Methods

2.1 Data set

This research made use of the SARS-CoV-CT dataset, which was available to the public and contained CT scan pictures from 1252 SARS-CoV-2 (COVID-19) patients and 1230 healthy controls (COVID-19). The data used to create the SARS-CoV CT dataset came from actual hospital patients in São Paulo, Brazil. Due to patient confidentiality, the hospital did not record each patient's specific characteristics. The dataset was accessed on Kaggle

dataset. There were 60 patients with a positive Covid test, 32 men and 28 women. Also considered were 60 patients who tested negative for Covid, 30 of whom were male and 30 of whom were female. Figure 1 displays some illustrative CT scan pictures taken from the dataset.

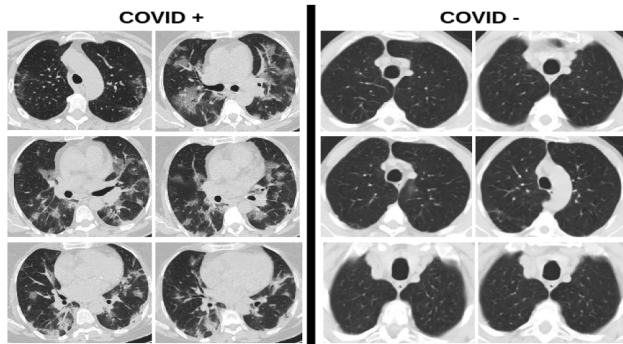


Figure 1. Representative chest CT scan images from the used dataset, including those of patients who tested positive and negative for COVID-19

2.2 Preprocessing of CT scan Images

We used the UM method to boost the high-frequency components of the grey level in the CT picture after downsampling the original photograph to a resolution of 100 by 100. (luminance). Unsharp masks are created by deconvolving a Gaussian blurred version of the original image. The edge-related high-frequency data can be found in the unsharp mask. Finally, an image is improved by adding a scaled mask to the source image.

The entropy image uses locally computed values from n by n blocks to quantify dissimilarity. Intensity distributions at a given location can be used to calculate entropy. The input entropy for the proposed bichannel CNN is shown in equation (1).

$$E_{\text{gray}} = - \sum_i P_{\text{gray}_{\text{UM}}}(i) \times \log_2 P_{\text{gray}_{\text{UM}}}(i) \quad (1)$$

where $P_{\text{gray}_{\text{UM}}}(i)$ represents, after UM processing, the frequency distribution of the i -th intensity inside a $n \times n$ block of the grey level component of the COVID image. For this reason, we use $n = 9$ to compute the entropy pictures of the grey level, as this yields the best accuracy compared to the other block sizes shown. The entropy pictures offer the local structural information of the CT scans using the statistical properties of the local locations.

2.3 Deep learning by bichannel CNN

The proposed bi-channel CNN architecture combined gray-level entropy and green channel (UM) images to enhance COVID-19 detection in lung CT scans. The architecture featured separate convolutional pipelines for each image type, followed by concatenation and dense layers for classification. The detailed design includes specific numbers of filters and activation functions to optimize feature extraction and classification performance. This comprehensive description provides a clear understanding of the model's structure and the rationale behind its design choices.

In this research, we employed a CNN to learn the features of referable CT. As shown in Figure 2, following UM processing, we built a grey level and green component entropy pictures simultaneously. In each of the four convolutional layers dedicated to a single channel, the number of filters increased from 32 to 64 to 128. Python and the TensorFlow library were used to implement the proposed approach of referable Covid detection. The model was trained using the Adam algorithm with a learning rate of 0.0001, and the cross-entropy loss function. Next is an explanation of how SSA was able to tune these hyper-parameters to their ideal values.

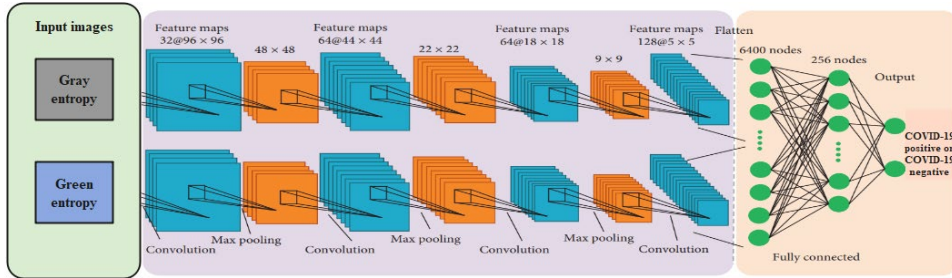


Figure 2. The diagram of the proposed bi-channel CNN model

2.4 Sparrow search algorithm (SSA)

There exists a well-defined mathematical model from which the sparrow search algorithm can be derived and constructed.

(1) The plenty of stamina show everyone where to scavenge and how to get there. Individual fitness levels are evaluated to determine the amount of energy available.

(2) When a predator is spotted, the sparrows sing to warn each other. When the alarm value exceeds the critical value, the producers must direct all survivors to a secure zone.

(3) Each sparrow has the potential to become a producer if it diligently seeks out the best food sources, but the ratio of creators to scavengers remains constant across the board. Many famished scavengers are more prone to travel great distances in search of food.

(4) In their quest to eat, the scavengers travel in the direction of the producer who can supply the best food.

(5) When danger is detected, the sparrows at the group's periphery make a beeline for the safe zone to improve their position, whereas the sparrows in the group's center simply stroll around at random to stay in close proximity to one another.

The experiment requires us to utilize digital sparrows to scavenge for virtual grubs. Matrices like as the one below can be used to depict sparrow locations.

$$X = \begin{bmatrix} X_{1,1} & X_{1,2} & \cdots & \cdots & X_{1,d} \\ X_{2,1} & X_{2,2} & \cdots & \cdots & X_{2,d} \\ \vdots & \vdots & \vdots & \vdots & \vdots \\ X_{n,1} & X_{n,2} & \cdots & \cdots & X_{n,d} \end{bmatrix} \quad (2)$$

where n is the total population of sparrows and d represents the depth of the optimization space. Thus, the following vector represents all sparrows' fitness values:

$$F_X = \begin{bmatrix} f([X_{1,1} & X_{1,2} & \dots & \dots & X_{1,d}]) \\ f([X_{2,1} & X_{2,2} & \dots & \dots & X_{2,d}]) \\ \vdots & \vdots & \vdots & \vdots & \vdots \\ f([X_{n,1} & X_{n,2} & \dots & \dots & X_{n,d}]) \end{bmatrix} \quad (3)$$

When the number of sparrows is represented by n and each sparrow's fitness is indicated by a row's value in F_X . Those SSA producers with higher fitness ratings are given preference during the food-finding procedure. In addition, producers are the ones who have to find food and direct the population's movements. Hence, unlike scavengers, producers have more options regarding where to look for food.

$$X_{i,j}^{t+1} = \begin{cases} X_{i,j}^t \cdot \exp\left(\frac{-i}{\alpha \cdot \text{iter}_{\max}}\right) & \text{if } R_2 < ST \\ X_{i,j}^t + Q \cdot L & \text{if } R_w \geq ST \end{cases} \quad (4)$$

Where t = current iteration, $j = 1, 2, \dots, d$. For each iteration, the value of the j th dimension of the i th sparrow is represented by $X_{i,j}^t$, where t is the iteration number. The maximum sum of iterations is denoted by the constant iter_{\max} . Numbers between zero and one are completely arbitrary. The alert value, represented by R_2 , ranges from $[0,1]$, while the safety threshold, ST , ranges from $[0.5,1.0]$. It is assumed that L represents a 1 by d matrix where all the cells contain the value 1.

Some freeloaders keep closer tabs on the manufacturers, as was described before. As soon as they learn the producer has discovered tasty food, they abandon their current location to go in search of sustenance. If they win, they can instantly obtain the producer's food; otherwise, rule enforcement will continue as planned in equation (5). The following is a description of the formula used to update the scrounger's position:

$$X_{i,j}^{t+1} = \begin{cases} Q \cdot \exp\left(\frac{X_{\text{worst}}^t - X_{i,j}^t}{i^2}\right) & \text{if } i > n/2 \\ X_P^{t+1} + |X_{i,j}^t - X_P^{t+1}| \cdot A^+ \cdot L & \text{otherwise} \end{cases} \quad (5)$$

where X_P is the best possible location for the manufacturer. The current worst place on Earth is denoted by X_{worst} . The matrix A has a size of 1 by d , and its elements are each either 1 or -1.

We suppose that between 10 and 20% of the sparrow population is alert to the threat in our simulation. A random number is used to determine where in the population each sparrow will start out.

$$X_{i,j}^{t+1} = \begin{cases} X_{\text{best}}^t + \beta \cdot |X_{i,j}^t - X_{\text{best}}^t| & \text{if } f_i > f_g \\ X_{i,j}^t + K \left(\frac{|X_{i,j}^t - X_{\text{worst}}^t|}{(f_i - f_w) + \epsilon} \right) & \text{if } f_i = f_g \end{cases} \quad (6)$$

where X_{best} is the best possible point in the world right now. The step size regulation K is a random number in the range $[-1,1]$. The top and worst fitness levels are denoted by f_g and f_w . To avoid the zero-division-error case, the smallest constant is ϵ is added.

To put it simply, if $f_i > f_g$, then the sparrow is on the periphery of the group. Sparrows can feel secure in and around the population center, which is denoted by X_{best} . The sparrows in the population's center are aware of the threat and need to congregate with the others,

as demonstrated by the equation $f_i=f_g$. The sparrow's movement direction is denoted by the letter K, which is also the step size control coefficient.

3. Results and Discussion

Accuracy in classification is measured as the ratio of right predictions to total data points. To determine precision, the equation (7) is used.

$$Acc = \frac{TP + TN}{TP + FP + TN + FN} \quad (7)$$

Where TP refers to the estimated accurate amount of data, FP refers to information that is harmful but misinterpreted as positive, TN refers to information that is actually damaging but misinterpreted as negative, and FN refers to information that is positive but misinterpreted as being unfavorable. The percentage of optimistic predictions that fall into the all-positive class is the degree of precision (positive predicted values in equation (8)).

$$prec = \frac{TP}{TP + FP} \quad (8)$$

Recall is calculated by taking the fraction of positive class elements that yield genuine positive (TP) results and dividing by the total number of such elements. Equation (9) provides the formula for determining the recall value:

$$Recall = \frac{TP}{TP + FN} \quad (9)$$

As a result of averaging the scores for accuracy and recall, we get the F1 score. Equation (10) demonstrates how to determine the F1 score:

$$F1 - measure = \frac{2 * prec * recall}{prec * recall} \quad (10)$$

In the accuracy analysis, the proposed model achieved 99.67%, the DBN and the LSTM achieved nearly 97%. Other models, including the CNN, RNN and GAN models, achieved nearly 98% accuracy. When the models were tested for precision, the existing replicas achieved around 97% to 98% and proposed model achieved 99.6%. In the analysis of F1-score, the existing models achieved around 97% to 98% and proposed model achieved 99.66%. Table 1, Figures 3 and 4 presents the graphical analysis of projected model in terms of numerous metrics.

Table 2 shows the analysis of various model for training and testing time. In this comparative analysis, we used different models. In Deep Belief Network (DBN), the training and the valid of $98.45 \pm 0.45\%$ and $95.14 \pm 0.70\%$ were achieved. Further, testing time was $94.67 \pm 1.28\%$ where the training time was 00:14:30. In addition, the test time was 00:00:03. In CNN, training was achieved at $99.56 \pm 0.41\%$ and the valid at $94.87 \pm 1.01\%$. In addition, the values for testing time, the training time, and the test time were $96.36 \pm 1.02\%$, 00:08:47 and 00:00:01, respectively. In RNN, the values of training, the valid, and testing time were $95.09 \pm 1.11\%$, $94.40 \pm 0.60\%$, and $94.80 \pm 1.68\%$, respectively, whereas the training time

Table 1. Comparative analysis of projected model for different metrics

Model	Accuracy	Precision	Recall	F1-Score
DBN	97.8	97.6	97.66	97.66
CNN	98.26	98	98.66	98.33
RNN	98.37	98.33	98.66	98.33
LSTM	97.91	97.66	98	97.66
GAN	98.60	98.33	98.66	98.33
Proposed Model	99.67	99.6	100	99.66

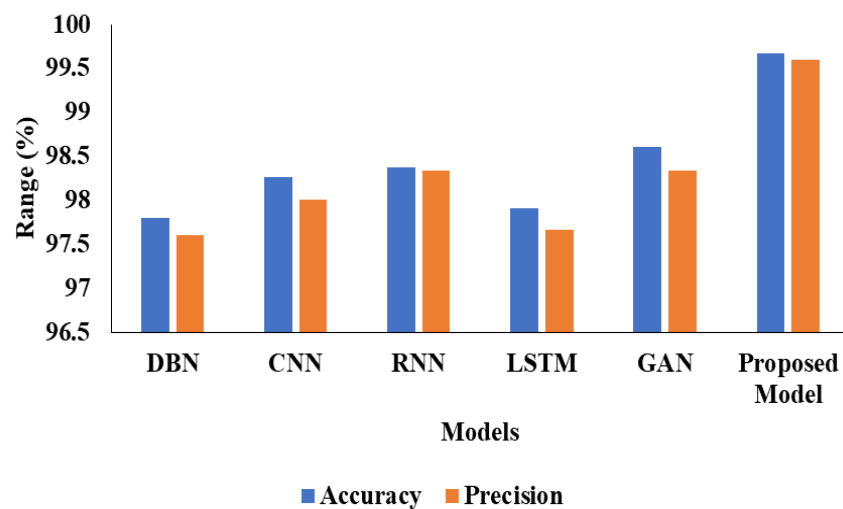
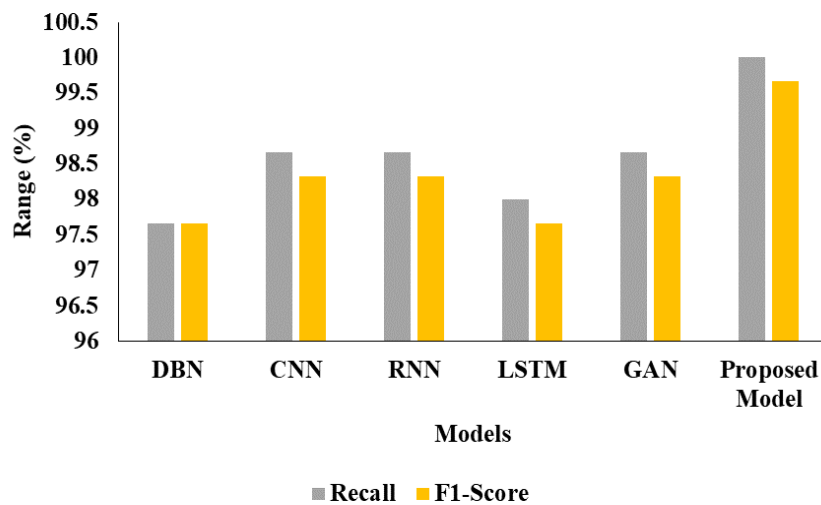
**Figure 3.** Analysis of proposed model**Figure 4.** Performance analysis of proposed model

Table 2. Analysis of various models for training and testing time

Model	Train	Valid	Test	Train Time	Test Time
DBN	98.45±0.45%	95.14±0.70%	94.67±1.28%	00:14:30	00:00:03
CNN	99.56±0.41%	94.87±1.01%	96.36±1.02%	00:08:47	00:00:01
RNN	95.09±1.11%	94.40±0.60%	94.80±1.68%	00:16:14	00:00:02
LSTM	99.75±0.14%	97.13±0.87%	94.81±0.58%	00:21:32	00:00:03
GAN	99.75±0.11%	98.10±0.66%	97.72±0.38%	00:12:23	00:00:03
Proposed Model	99.88±0.07%	97.62±0.64%	97.13±0.86%	00:09:20	00:00:02

was achieved at 00:16:14 and the test time was 00:00:02. In LSTM, the testing time was 94.81±0.58%, the training time was 00:21:32, and the test time was 00:00:03. In GAN (generative adversarial network), the values of training, the valid, and testing time were 99.75±0.11%, 98.10±0.66%, and 97.72±0.38%, respectively, whereas the values of the training time and the test time were 00:12:23 and 00:00:03, respectively. As per proposed model, training was achieved at 99.88±0.07% where the valid and testing time were at 97.62±0.64% and 97.13±0.86%. The values of training time and the test time were 00:09:20 and 00:00:02, respectively. The results in this analysis showed that the proposed model gave better results when compared to other models.

In this study, a novel approach for detecting lung infections on CT scans in COVID-19 patients utilizing the Sparrow Search Based Deep Learning model was introduced. The method demonstrated promising results in terms of accuracy and sensitivity, as evidenced by the findings presented in Table 1 and Figures 3 and 4. However, a deeper study of the model's interpretability and generalizability is needed to fully assess its robustness across diverse patient populations and imaging settings. Furthermore, while these initial experiments show encouraging outcomes, additional validation through larger-scale trials and comparative studies with established diagnostic methods is essential to establish its clinical utility. Addressing these aspects will not only enhance confidence in the proposed approach but also pave the way for its potential integration into clinical practice, thereby improving early detection and treatment outcomes for COVID-19-related lung infections.

4. Conclusions

The proposed method relieves radiologists' workload by facilitating cross-verification of testing kit results. As a result of this proposed work, countries will be able to conduct more tests than have previously been possible. Future research in other areas where CT scans or other frequency-oriented data plays an important role will be motivated to adopt this unique approach. When it comes to identifying and diagnosing COVID in patients, a deep learning system can improve detection and diagnosis accuracy. In order to improve the precision, sensitivity, and specificity of a detection system, UM pre-processing is often employed. UM's grey level entropy images and a second independent CNN input were both used to improve the detection of recognizable COVID-19. The CNN's classification accuracy was superior to those of competing models thanks to the SSA optimization of the

learning rate of CNN. Our results demonstrate that our proposed method was successful in enhancing the model's performance using the same deep learning methods. To summarize, the proposed bi-channel CNN for detecting COVID-19 lung images demonstrated significant potential for aiding radiologists in diagnosis. The model's high accuracy and low false-negative rate indicated its efficacy in clinical settings. However, there are several avenues for future work. First, expanding the dataset to include more diverse samples could further enhance model robustness and generalizability. Additionally, integrating other image processing techniques and exploring multi-channel approaches could potentially improve performance. Finally, implementing the model in real-time clinical settings and conducting prospective studies would validate its practical applicability and impact on patient outcomes.

5. Conflicts of Interest

There is no conflict of interest.

ORCID

Kannadhasan Suriyan  <https://orcid.org/0000-0001-6443-9993>

References

Alhares, H., Tanha, J., & Balafer, M. A. (2023). AMTLDC: A new adversarial multi-source transfer learning framework to diagnosis of COVID-19. *Evolving Systems*, 15(2), 1-15.

Asnaoui, K. E., & Chawki, Y. (2021). Using X-ray images and deep learning for automated detection of coronavirus disease. *Journal of Biomolecular Structure and Dynamics*, 39(10), 3615-3626. <https://doi.org/10.1080/07391102.2020.1767212>

Attallah, O., & Samir, A. (2022). A wavelet-based deep learning pipeline for efficient COVID-19 diagnosis via CT slices. *Applied Soft Computing*, 128 (2), Article 109401. <https://doi.org/10.1016/j.asoc.2022.109401>

Bhattacharyya, A., Bhaik, D., Kumar, S., Thakur, P., Sharma, R., & Pachori, R. B. (2022). A deep learning based approach for automatic detection of COVID-19 cases using chest X-ray images. *Biomedical Signal Processing and Control*, 71(2), Article 103182. <https://doi.org/10.1016/j.bspc.2021.103182>

Biradar, V. G., Pareek, P. K., Vani, K. S., & Nagarathna, P. (2022). Lung cancer detection and classification using 2d convolutional neural network. In *Proceeding of the 2022 IEEE 2nd Mysore Sub Section International Conference (MysuruCon)* (pp. 1-5). IEEE. <https://doi.org/10.1109/MysuruCon55714.2022.9972595>

Diaz-Escobar, J., Ordóñez-Guillén, N. E., Villarreal-Reyes, S., Galaviz-Mosqueda, A., Kober, V., Rivera-Rodriguez, R., & Rizk, J. E. L. (2021). Deep-learning based detection of COVID-19 using lung ultrasound imagery. *PLoS ONE*, 16(8), Article e0255886. <https://doi.org/10.1371/journal.pone.0255886>

Gupta, K., & Bajaj, V. (2023). Deep learning models-based CT-scan image classification for automated screening of COVID-19. *Biomedical Signal Processing and Control*, 80(Part 1), Article 104268. <https://doi.org/10.1016/j.bspc.2022.104268>

Hussain, E., Hasan, M., Rahman, M. A., Lee, I., Tamanna, T., & Parvez, M. Z. (2021). CoroDet: A deep learning-based classification for COVID-19 detection using chest X-ray images. *Chaos, Solitons & Fractals*, 142(7), Article 110495. <https://doi.org/10.1016/j.chaos.2020.110495>

Jain, R., Gupta, M., Taneja, S., & Hemanth, D. J. (2021). Deep learning based detection and analysis of COVID-19 on chest X-ray images. *Applied Intelligence*, 51(5), 1690-1700.

Kailasam, S., Achanta, S. D. M., Rao, P. R. K., Vatambeti, R., & Kayam, S. (2022). An IoT-based agriculture maintenance using pervasive computing with machine learning technique. *International Journal of Intelligent Computing and Cybernetics*, 15(2), 184-197. <https://doi.org/10.1108/IJICC-06-2021-0101>

Kasthuri, L. J. S., & Jebaseeli, A. N. (2018). A robust data classification in online social networks through automatically mining query facts. *International Journal of Scientific Research in Computer Science Applications and Management Studies*, 7(4), 1-4.

Kathamuthu, N. D., Subramaniam, S., Le, Q. H., Muthusamy, S., Panchal, H., Sundararajan, S. C. M., Alrubaie, A. J., & Zahra, M. M. A. (2023). A deep transfer learning-based convolution neural network model for COVID-19 detection using computed tomography scan images for medical applications. *Advances in Engineering Software*, 175(5), Article 103317. <https://doi.org/10.1016/j.advengsoft.2022.103317>

Kordnoori, S., Sabeti, M., Mostafaei, H., & Banihashemi, S. S. A. (2023). Analysis of lung scan imaging using deep multi-task learning structure for Covid-19 disease. *IET Image Processing*, 15(2), 1581-1588.

Motwani, A., Shukla, P. K., Pawar, M., Kumar, M., Ghosh, U., Alnumay, W., & Nayak, S. R. (2023). Enhanced framework for COVID-19 prediction with computed tomography scan images using dense convolutional neural network and novel loss function. *Computers and Electrical Engineering*, 105(2), Article 108479. <https://doi.org/10.1016/j.compeleceng.2022.108479>

Nayak, S. R., Nayak, D. R., Sinha, U., Arora, V., & Pachori, R. B. (2021). Application of deep learning techniques for detection of COVID-19 cases using chest X-ray images: A comprehensive study. *Biomedical Signal Processing and Control*, 64(5), Article 102365. <https://doi.org/10.1016/j.bspc.2020.102365>

Rehman, A., Iqbal, M. A., Xing, H., & Ahmed, I. (2021). COVID-19 detection empowered with machine learning and deep learning techniques: A systematic review. *Applied Sciences*, 11(8), Article 3414. <https://doi.org/10.3390/app11083414>

Sadhana, S., Pandiarajan, S., Sivaraman, E., & Daniel, D. (2021). AI-based power screening solution for SARS-CoV2 infection: A sociodemographic survey and COVID-19 cough detector. *Procedia Computer Science*, 194(2), 255-271. <https://doi.org/10.1016/j.procs.2021.10.081>

Subramanian, N., Elharrouss, O., Al-Maadeed, S., & Chowdhury, M. (2022). A review of deep learning-based detection methods for COVID-19. *Computers in Biology and Medicine*, 143, Article 105233. <https://doi.org/10.1016/j.combiomed.2022.105233>

Swapna, M., Viswanadhula, U. M., Aluvalu, R., Vardharajan, V., & Kotecha, K. (2022). Bio-signals in medical applications and challenges using artificial intelligence. *Journal of Sensor and Actuator Networks*, 11(1), Article 17. <https://doi.org/10.3390/jsan11010017>

Venaktesh, C., Ramana, K., Lakkisetty, S. Y., Band, S. S., Agarwal, S. & Mosavi, A. (2022). A neural network and optimization based lung cancer detection system in CT images. *Frontiers in Public Health*, 10, Article 769692. <https://doi.org/10.3389/fpubh.2022.769692>

Yang, D., Martinez, C., Visuña, L., Khandhar, H., Bhatt, C. & Carretero, J. (2021). Detection and analysis of COVID-19 in medical images using deep learning techniques. *Scientific Reports*, 11(1), Article 19638. <https://doi.org/10.1038/s41598-021-99015-3>